

Electronic Supplementary Information

Highly Flexible, Freestanding Tandem Sulfur Cathodes for Foldable Li-S Batteries with High Areal Capacity

*Chi-Hao Chang, Sheng-Heng Chung, and Arumugam Manthiram**

C.-H. Chang, S.-H. Chung, Prof. A. Manthiram

Materials Science and Engineering Program & Texas Materials Institute

The University of Texas at Austin, Austin, TX 78712, USA

E-mail: manth@austin.utexas.edu (A. Manthiram)

Fabrication of tandem cathodes: The tandem cathode was fabricated via a one-step vacuum-filtration method. For the purpose of simplifying the fabrication processes, the tandem sulfur cathode could be fabricated directly by commercial single-wall nanotubes (SWCNT, Tuball), carbon nanofibers (CNF, Pyrograf Products, Inc.), and micro-sized commercial sulfur (S, Fisher Scientific; purity = 99.5 %) without binder addition and additional modification. In other words, the tandem cathode appears superior in cost and simplicity to the conventional cathodes involving the nanocomposite approach and the slurry-coating method. In detail, the SWCNT/CNF mixtures (the mass ratio is 1 : 10) and CNF/S mixtures (the mass ratio is 1 : 4) (Table S2) were dispersed in sulfur-saturated isopropyl alcohol (IPA) solutions. After ultrasonication, the well-suspended SWCNT/CNF mixtures were vacuum filtrated through a filter paper (Filter paper P5 grade, Fisher Scientific) with a diameter of 9 cm as the SWCNT/CNF conductive layer. Subsequently, the CNF/S solution was directly vacuum filtrated onto the SWCNT/CNF thin film as the CNF/S active-material layer. The resulting tandem cathode with 4 mg cm⁻² sulfur was peeled off from the filter paper and dried in an oven for 24 h at 50 °C. To further increase the sulfur loading, the integration of the LBL technique was utilized to fabricate tandem cathodes with various sulfur loadings (8, 12, and

16 mg cm⁻²) by the same vacuum-filtration process. The prepared cathodes were roll-pressed and then cut into discs with an area of 1.13 cm². The thicknesses are approximately 100, 200, 300, and 400 μm for tandem cathodes with, respectively, 4, 8, 12, and 16 mg cm⁻² sulfur. The corresponding bulk density is 0.59 g cm⁻³.

Cell configuration of Li-S cells using tandem cathodes: The cathodes with different loadings were dried in an oven at 50 °C for 1 hour to remove moisture before assembling the cells. The prepared cathode, separator (Celgard 2500, Celgard), and Li foil (Aldrich) were placed in CR2032-type coin cell inside an argon-filled glove box. The cathodes with different sulfur loadings were assembled with the SWCNT/CNF conductive layer facing the Li anode. 1.85 M lithium trifluoromethanesulfonate (LiCF₃SO₃, Acros Organics) and 0.1 M additive lithium nitrate (LiNO₃, Acros Organics) were dissolved in 1,2-dimethoxyethane (DME, Acros Organics)/1,3-dioxolane (DOL, Acros Organics) co-solvent (1:1 volume ratio) as the standard electrolyte. The electrolyte to sulfur (E/S) ratio for all Li-S coin cells is fixed to 15 :1 which is the common value in the recently published reports.

Preparation of conventional cathodes: The conventional cathodes were fabricated by casting the active-material slurry onto an Al foil current collector. The casted cathodes were dried in an oven at 50 °C for 48 h. The active-material slurry used in this work composed of 60 wt.% S, 20 wt.% PVdF, and 20 wt.% Super P (TIMCAL). Only the conventional cathodes with 3 mg cm⁻² sulfur were tested in this work because the conventional cathode with higher sulfur loadings would form numerous cracks. Moreover, the active-material coating would easily peel off from the Al foil if the loading increased to 4 mg cm⁻² (Fig. S1a).

Assemble of control Li-S cells: The procedure for assembling the conventional Li-S cells is almost the same as the experimental Li-S cells employing the tandem cathodes except for

using the conventional cathodes. The same standard electrolyte was used in the control cells as well. The E/S ratio is fixed to 15 : 1 which is the same as that of Li-S cells employing tandem cathodes.

Assembly of Foldable Li-S batteries: The foldable Li-S cells were assembled with the same electrolyte. Unlike patented cathodes used in the previous foldable cells,¹ the tandem cathode was cut into 2 x 6 cm² and directly used as the cathode in the foldable Li-S battery without requiring other processes. This is because the tandem cathode has excellent mechanical stability to sustain the folding deformation. Celgard 2500 was used as the separator to avoid cell shorts. The cells were sealed with an aluminum soft packaging film. The foldable Li-S battery possesses the highest sulfur loading of 16 mg cm⁻² sulfur (sulfur mass in entire cathode: 192 mg) so far. The E/S ratio was decreased to ~10 in order to prevent the electrolyte being squeezed out during the folding processes. The cells were rested for 6 h before the electrochemical examinations. The whole test conditions are the same as that for the coin cells.

Polysulfide-trapping test: The carbon-based tandem cathodes without sulfur particles were fabricated to examine the polysulfide-trapping capabilities. The fabrication process is the same except for no sulfur addition. To test the polysulfide-trapping ability, the tandem cathode was placed onto the separator. Then 250 μ L of 0.38 M polysulfides (Li₂S₆) (corresponding to 18.24 mg sulfur) synthesized by reacting S and Li₂S was poured onto the tandem cathode. Subsequently, the tandem cathode was stored for 8 h. The entire experiment was conducted inside an Ar-filled glove box.

Materials characterizations: The microstructure of the cathodes before and after cycling were investigated with a field emission scanning electron microscope (FE-SEM) (Quanta 650

FESEM, FEI) with an energy dispersive X-ray spectrometer (EDX) for recording elemental signals and mapping and line-scanning the results. The cycled cathodes including the tandem cathode and the conventional cathode were collected from the Li-S cells (at the charged state, 2.8 V) after 100 cycles that were disassembled inside an argon-filled glove box. The retrieved cathodes were cleaned with the DOL/DME co-solvent (1:1 volume ratio) twice and the residual co-solvent was carefully removed by Kimwipes. The SEM samples were transferred by a well-sealed glass sample vial filled with argon to avoid exposure to air. To scrutinize the inner-areas of the cycled integrated cathode, the SWCNT/CNF layer was carefully removed. The cross-sectional samples were prepared by cutting fresh and cycled tandem cathodes with a Gillette blade. The tandem cathodes remained with extremely good mechanical strength before or after cycling. Therefore, the cross-sectional samples need to be torn apart to show the cross-section surface. The cutting and tearing processes, as a result, might slightly damage the cross-sections of the tandem cathodes.

Electrochemical measurements: The as-assembled Li-S cells were rested for 30 min at ambient temperature before the electrochemical measurements. An impedance analyzer (SI 1260, Solartron) was used to collect the electrochemical impedance spectra (EIS) in the frequency range of 1 MHz to 100 mHz. The cyclic voltammetry (CV) measurement was conducted with a universal potentiostat (VoltaLab PGZ 402, Radiometer Analytical) between 1.7 and 2.8 V at 0.1 mV s^{-1} . In the CV test, we used the integrated cathode with 4 mg cm^{-2} sulfur as a demonstration. Discharge/charge profiles and cycling performances were recorded with an Arbin test station. All discharge capacities were calculated based on the mass and the theoretical capacity of sulfur. Foldable Li-S batteries were tested in the same discharge/charge conditions. The foldable cells were carefully folded to different angles (original, 90° , 180° , and recovered) and examined under the respective states for 2 discharge/charge cycles.

Supplementary Figures and Tables

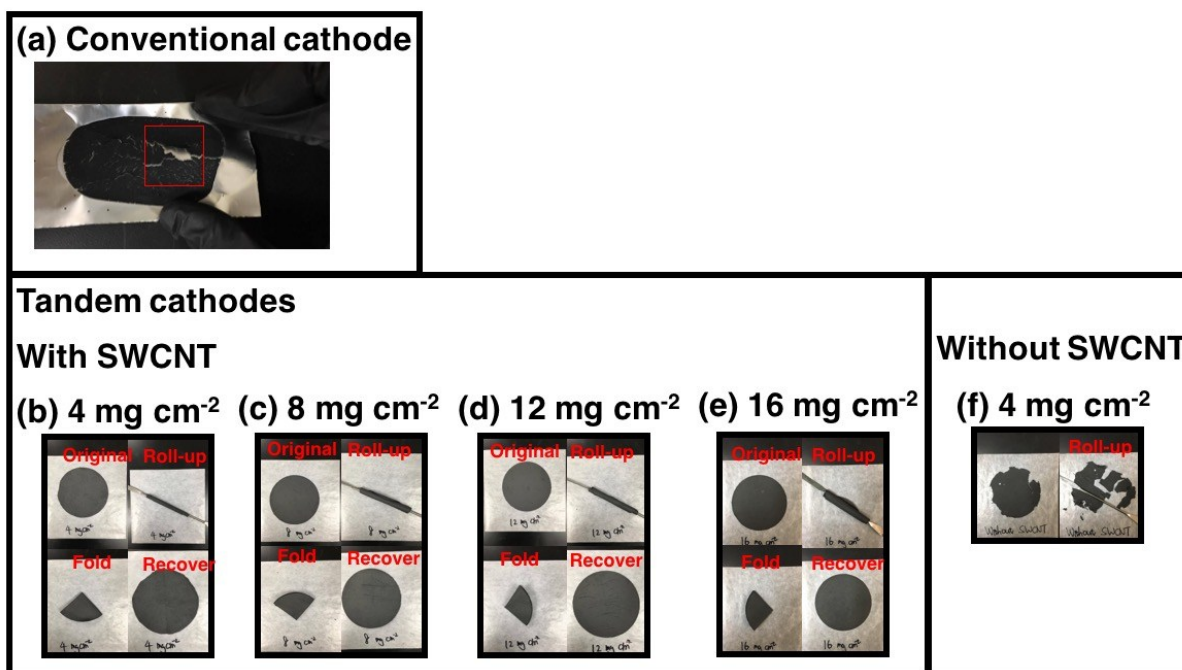


Fig. S1 (a) The conventional cathode with high sulfur loadings. (b - e) Cathodes with the SWCNT framework and (f) the tandem cathodes without SWCNT as the supporting framework.

The mechanical properties of the cathodes with and without the SWCNT framework are shown in Fig. S1. Fig. S1a shows that the cathodes without the SWCNT as the backbone exhibit poor mechanical properties. They are unable to be peeled off easily from the filter papers and cannot bear any mechanical tests (*e.g.*, roll up to form a cylinder). After being rolled up, they were unable to recover to their original shape and failed to retain the cathode integrity,

On the contrary, the tandem cathodes with the SWCNT backbone attained extraordinary mechanical properties. Fig. S1b - e exhibits that the tandem cathodes were able to recover to their original shape with a smooth surface and a well-retained cathode integrity after being rolled around the spatula to form a cylindrical structure and being multi-folded. The outstanding mechanical flexibility and strength proved here suggest that the cathodes with the SWCNT framework effectively tolerates the devastating force from the volume

change caused by the sulfur-Li₂S conversion, ensuring their normal functions in the cell during cycling. More importantly, the high flexibility of the tandem cathodes provides a potential to prepare foldable Li-S batteries.

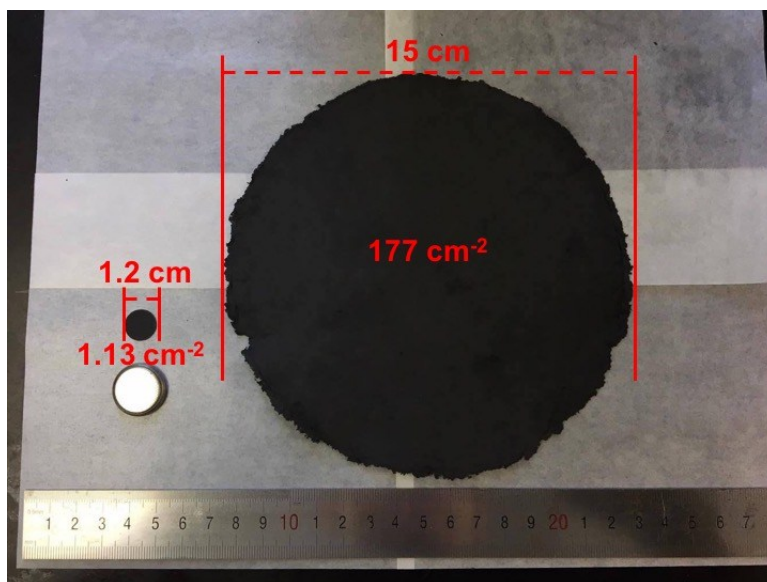


Fig. S2 The large-scale tandem sulfur cathode with 16 mg cm⁻² sulfur.

Fig. S2 shows that the flexible tandem cathode can be easily scaled up to a large size with an area of 177 cm², which is 157-time larger than that of tandem cathode used in the coin cell, by using the same vacuum-filtration process through a larger filter paper (177 cm²). In other words, the tandem cathode is amenable to large-scale fabrication.

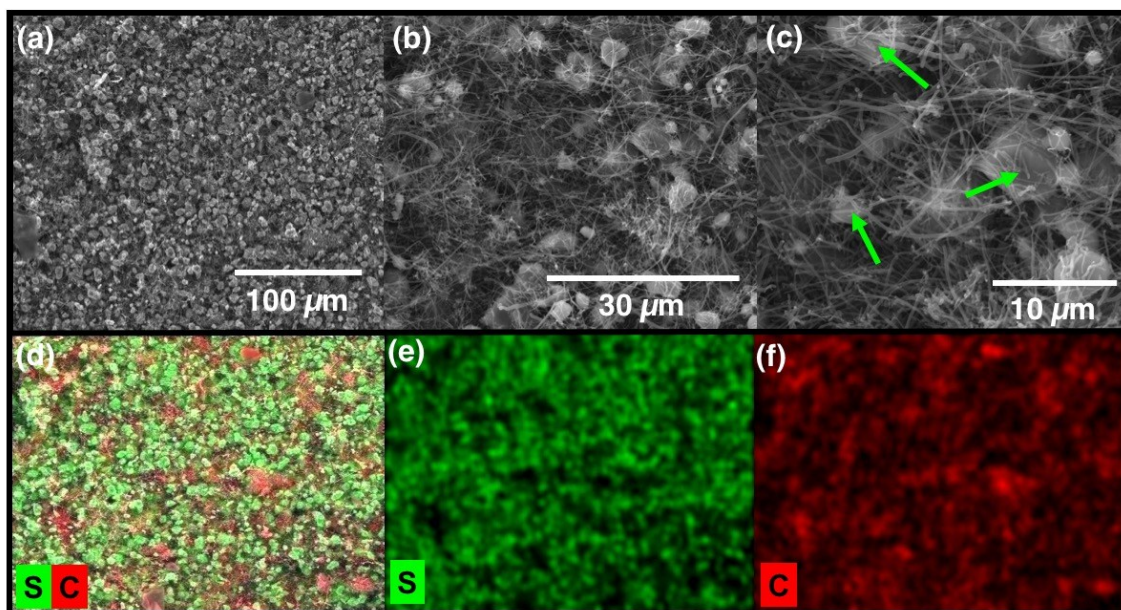


Fig. S3 Surface SEM inspection: (a - c) uncyclized CNF/S active-material layer and (d - f) EDX mapping results of (a).

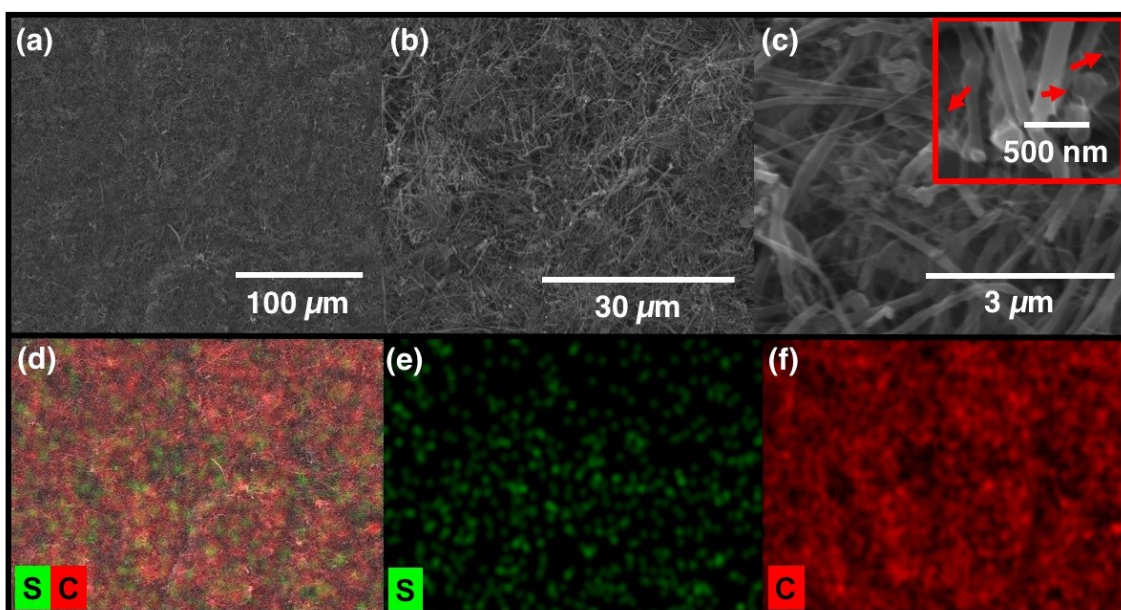


Fig. S4 Surface SEM inspection: (a - c) uncyclized SWCNT/CNF conductive layer and (d - f) EDX mapping results of (a).

The different morphologies between the CNF/S active-material layer and the SWCNT/CNF conductive layer are, respectively, shown in Fig. S3 – S4. Fig. 3 shows that a huge amount of sulfur particles with an average diameter of 5 – 10 μm (green arrows in Fig. S3c) is embedded in the interconnected CNF web. In sharp contrast, no noticeable sulfur

particles can be found in the SWCNT/CNF layer (Fig. S4). Moreover, the long SWCNTs (width: 2 – 3 nm; length: > 5 μm , red arrows in the inset of Fig. S4c) were self-weaved with the CNFs (width: 150 nm; length: 50 – 100 μm) to form interconnected porous structures, which offer polysulfides the herculean migration routes.^{S2} The comparison between these two layers reveals that the strong sulfur signals was only found in the CNF/S layer. This indicates that the CNF matrix well encapsulates the active sulfur particles within its porous framework. In contrast, the SWCNT/CNF layer is initially free of sulfur before cycling and would be able to cease the possible polysulfide diffusion.

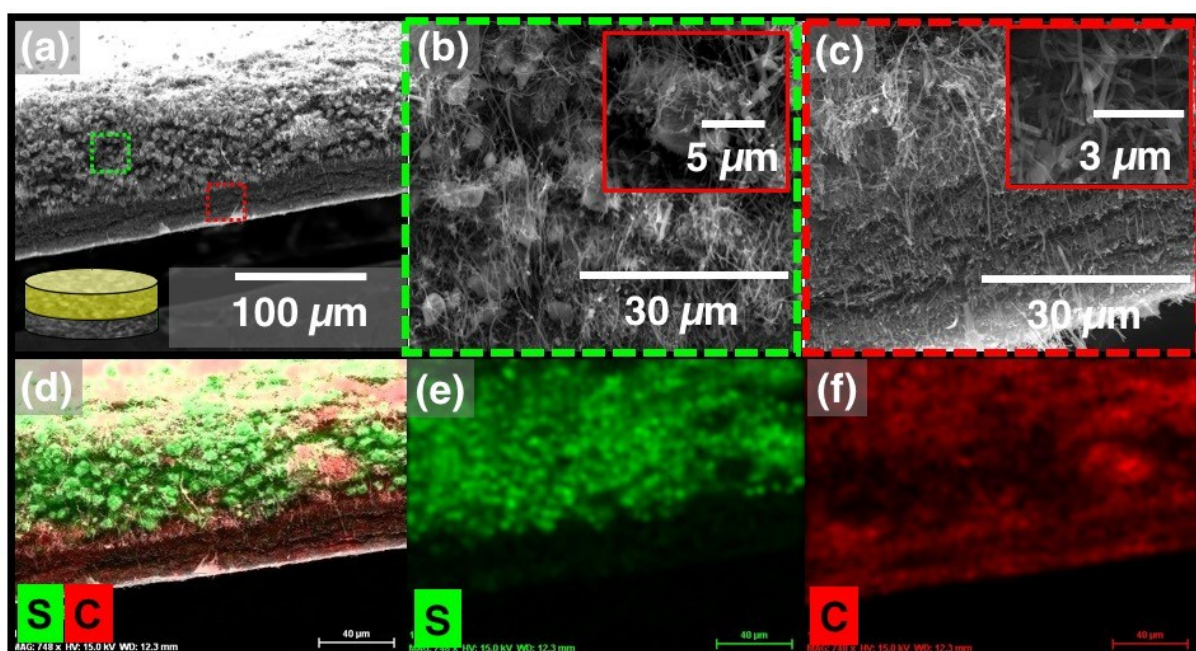


Fig. S5 Cross-sectional SEM inspection of the uncycled tandem cathodes (sulfur loading is 4 mg cm^{-2}): (a) uncycled tandem cathode, (b) CNF/S active-material layer, and (c) SWCNT/CNF conductive layer. (d – f) EDX mapping results of (a).

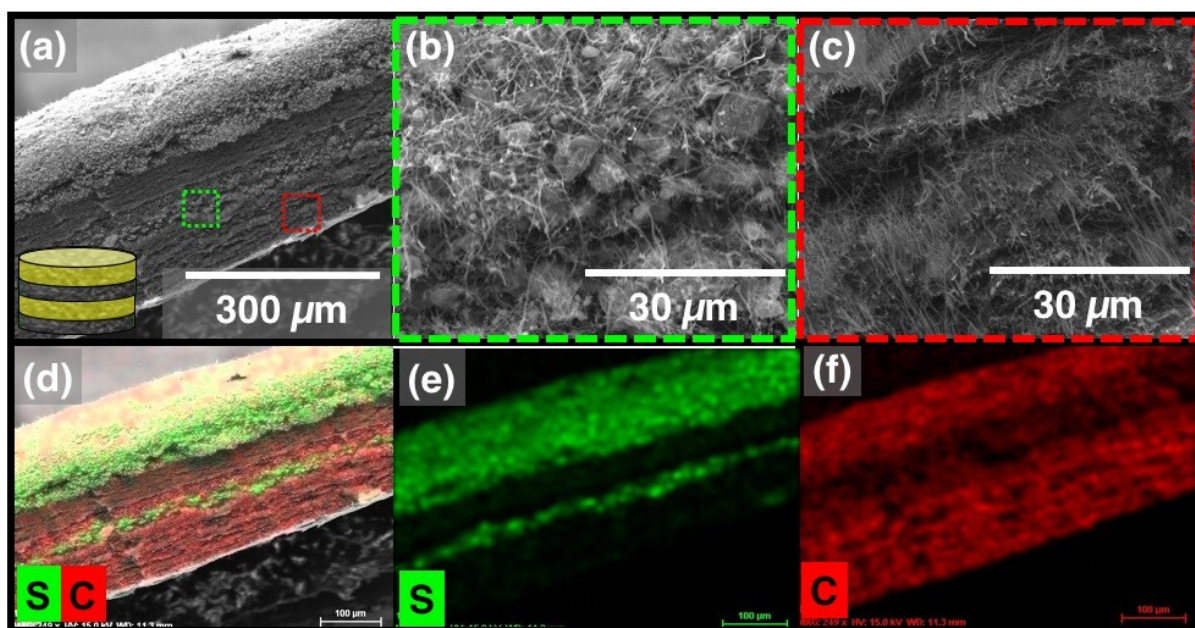


Fig. S6 Cross-sectional SEM inspection of the uncycled tandem cathodes (sulfur loading is 8 mg cm⁻²): (a) uncycled tandem cathode, (b) CNF/S active-material layer, and (c) SWCNT/CNF conductive layer. (d – f) EDX mapping results of (a).

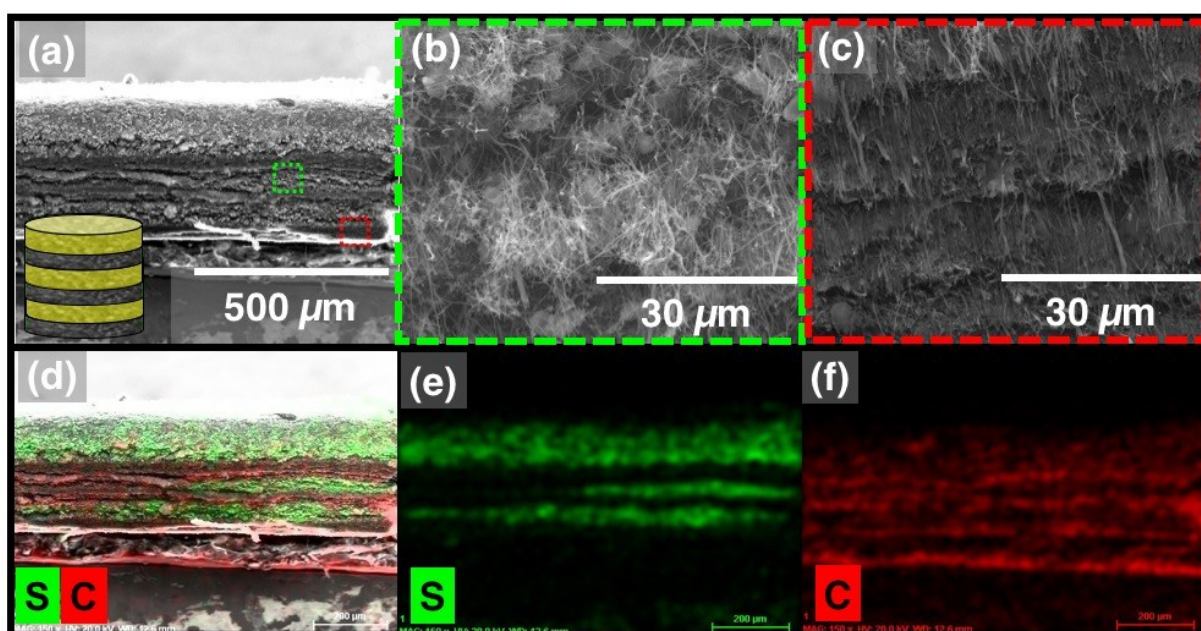


Fig. S7 Cross-sectional SEM inspection of the uncycled tandem cathodes (sulfur loading is 12 mg cm⁻²): (a) uncycled tandem cathode, (b) CNF/S active-material layer, and (c) SWCNT/CNF conductive layer. (d – f) EDX mapping results of (a).

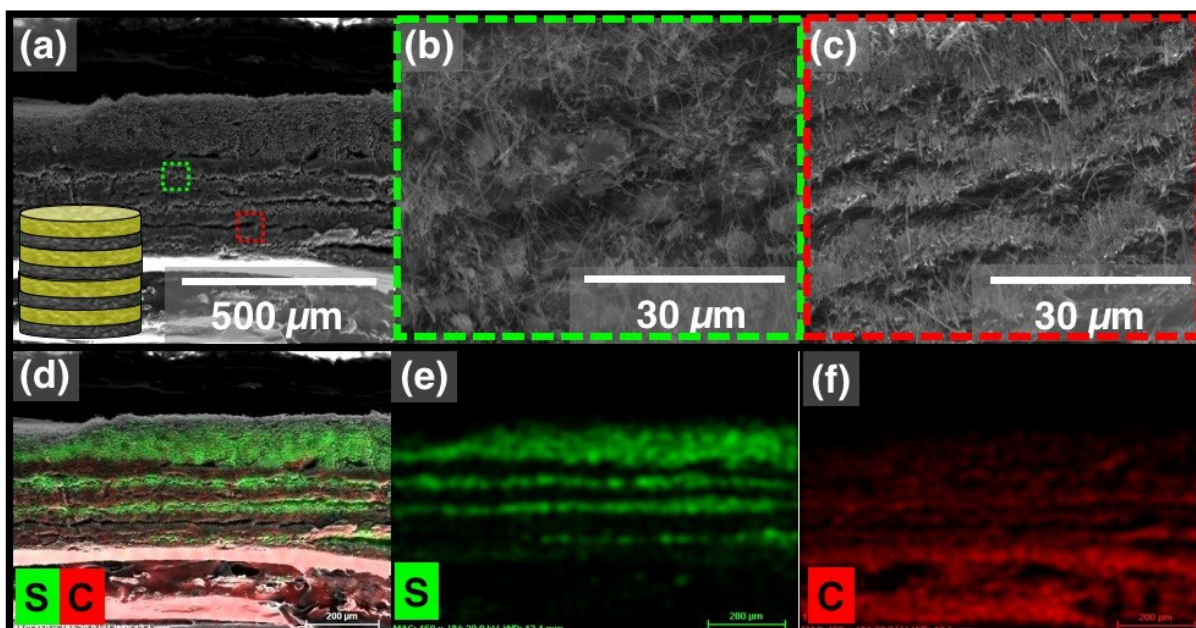


Fig. S8 Cross-sectional SEM inspection of the uncycled tandem cathodes (sulfur loading is 16 mg cm^{-2}): (a) uncycled tandem cathode, (b) CNF/S active-material layer, and (c) SWCNT/CNF conductive layer. (d – f) EDX mapping results of (a).

The cross-sectional SEM images and the elemental mapping/line-scanning results of the tandem cathodes with the sulfur loading of 4 mg cm^{-2} are, respectively, shown in Fig. S5. We can easily distinguish the CNF/S active-material layer and the SWCNT/CNF conductive layer in Fig. S5a – c because of the obvious morphological differences. In the CNF/S layer, the sulfur particles were tightly entangled by the conductive CNF network. The intimate contact between the insulating active material and the conductive CNFs could be the crux for developing high loading sulfur cathodes with an efficient electrochemical utilization. On the other hand, in the SWCNT/CNF conductive layer, the SWCNTs and CNFs were intertwined together and formed porous architectures. Such a porous SWCNT/CNF layer with conductive carbon skeleton could first trap the diffusing polysulfide and then transfer ions and electrons to re-activate the trapped active material.

In Fig. S5d – e, the CNF/S layer and the SWCNT/CNF layer can be identified from the elemental mapping and line-scanning results. The extremely strong elemental sulfur

signals (green) were found in the CNF/S active-material layer rather than in the SWCNT/CNF conductive layer. This reaffirms the different functions between the CNF/S active-material layer and the SWCNT/CNF conductive layer, which are to hold/store the active material and trap/prevent the polysulfide diffusion.

The SEM images and the corresponding elemental mapping results of the freestanding tandem cathodes with 8, 12, and 16 mg cm⁻² sulfur are, respectively, shown in Fig. S6 – S8. Each CNF/S layer and SWCNT/CNF layer could also readily be distinguished in the freestanding tandem cathodes. We can observe that 2, 3, and 4 CNF/S and SWCNT/CNF layers, respectively, in the tandem cathodes with sulfur loadings of 8, 12, and 16 mg cm⁻². Moreover, each CNF/S active-material layer exhibits the same morphology showing that sulfur particles are homogeneously dispersed in the CNF matrix and were tightly entangled by the conductive CNFs. In each SWCNT/CNF conducting layer, the interconnected porous structure is very similar.

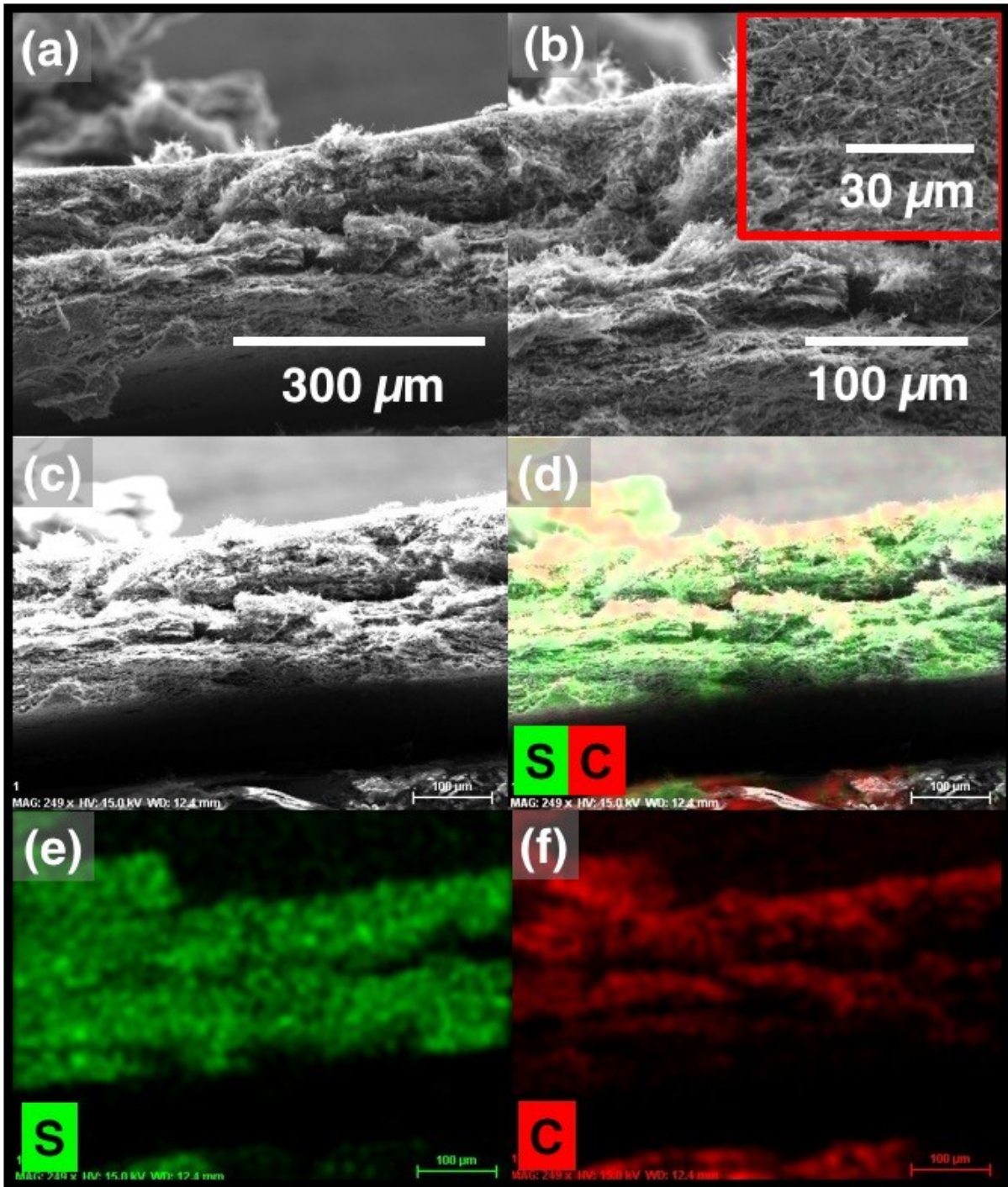


Fig. S9 (a - c) Cross-sectional SEM inspection and (d - f) the corresponding elemental mapping results of the cycled tandem cathodes (sulfur loading is 8 mg cm^{-2}) after 100 cycles.

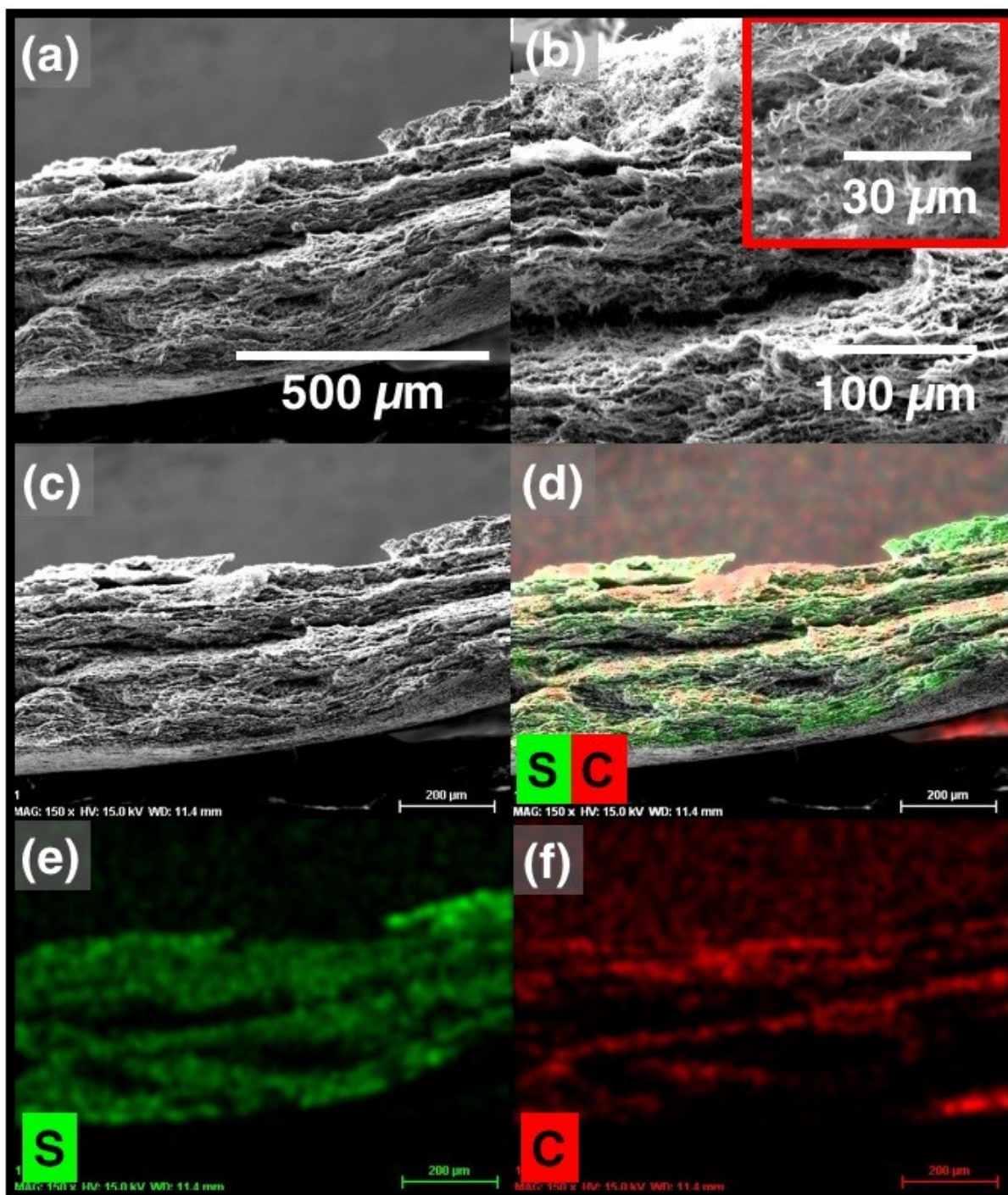


Fig. S10 (a - c) Cross-sectional SEM inspection and (d - f) the corresponding elemental mapping results of the cyclized tandem cathodes (sulfur loading is 12 mg cm^{-2}) after 100 cycles.

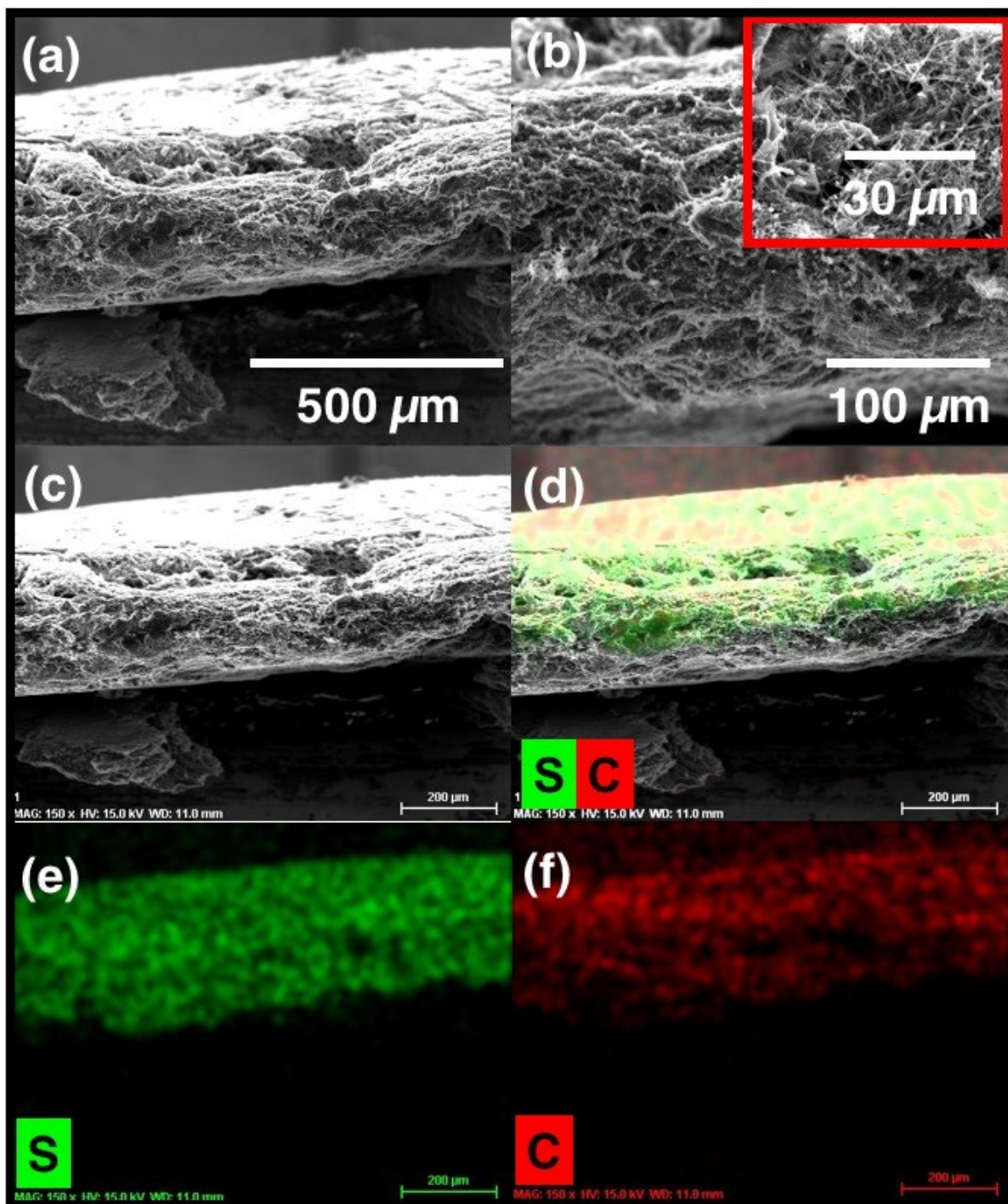


Fig. S11 (a - c) Cross-sectional SEM inspection and (d - f) the corresponding elemental mapping results of the cyclized tandem cathodes (sulfur loading is 16 mg cm^{-2}) after 100 cycles.

After 100 discharge/charge operations, the cyclized tandem cathodes were terminated at the fully charged state for the SEM/EDX investigation for detect the morphological and

elemental changes after cycling. As shown in the series of microstructure analysis (Fig. S9 - 11), the microstructure and elemental analysis demonstrate that the tandem cathodes remain the same with interconnected fibrous architectures with numerous physical spaces, reaffirming the statement that the tandem cathodes have higher tolerance to bear the mechanical stress stemmed from the conversion reaction between S and sulfide. The conductive carbon framework, including the CNFs and SWCNT/CNFs, provides smooth electron pathway and the porous network provides interconnected electrolyte channels, which can continuously reutilize the trapped active material immobilized within the tandem cathodes.^{S3} After long cycling, the elemental mapping result indicates the rearrangement of the active material in the tandem cathodes, implying that the reacted active material can rearrange and reside in the electrochemically preferred sites. This could, therefore, decrease the internal resistance. A more detailed discussion is summarized in Fig. S14a – c.^{S4, S5}

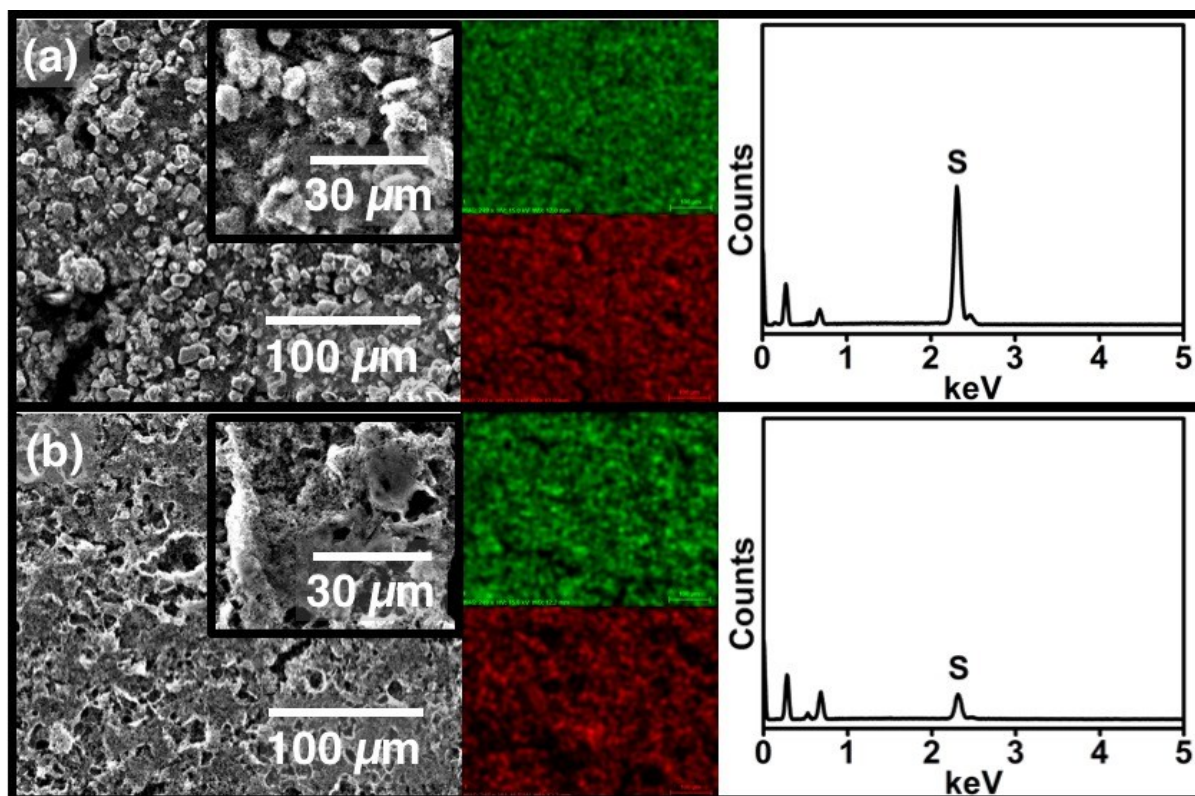


Fig. S12 The SEM images and elemental mapping results of the conventional cathode (a) before and (b) after cycling.

Fig. S12 shows the huge difference in the conventional sulfur cathode before and after cycling. Before cycling, large sulfur particles (5 – 10 μm) are clearly observed in the conventional sulfur cathode. However, the conventional cathode after cycling possesses large voids which are due to the dissolution of the active material. The dramatic decrease in the sulfur signals shown in the elemental mapping after the cycling also confirms the severe polysulfide migration in the conventional sulfur cathode. It can be observed that the insulating precipitates deposit onto the surface of the cycled conventional cathode, deteriorating the electrochemical performance.

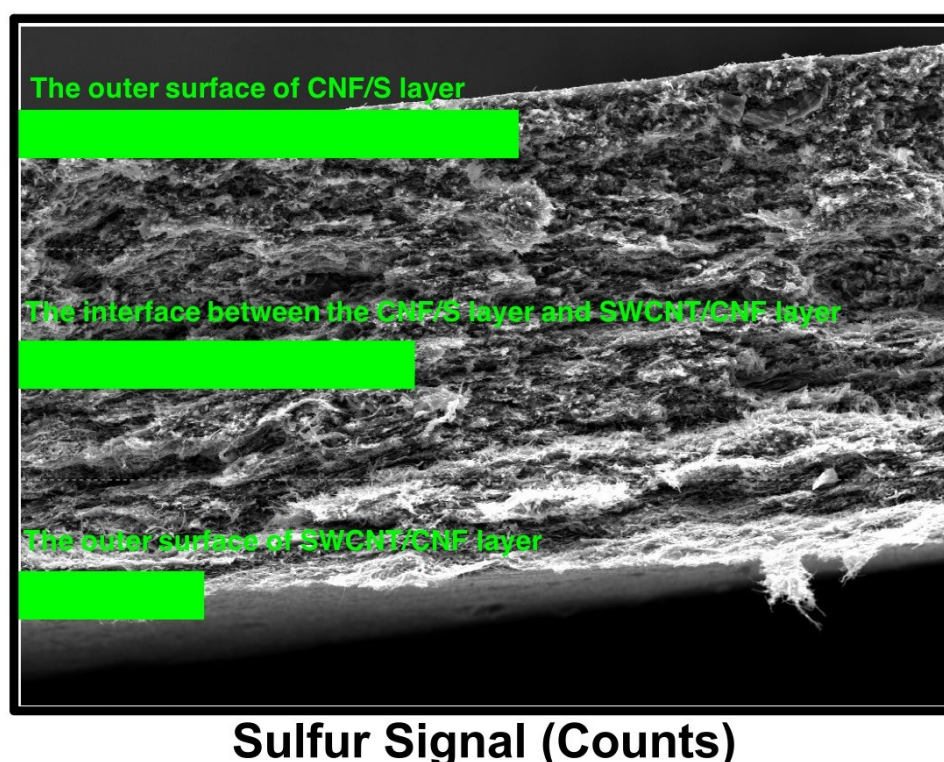


Fig. S13 Sulfur-signal-intensity gradients in the cycled tandem cathode.

The apparent sulfur-signal-intensity gradients reaffirm the functions of retarding polysulfide migration in tandem cathodes (Fig. S13): (i) CNF matrices in CNF/S layers act as

the reservoir to store the majority of polysulfides, (ii) SWCNT/CNF layers with porous structures serve as (a) puzzle-like polysulfide migration routes, which effectively prolong their migration time and (b) polysulfide traps which confine the migrating polysulfides.

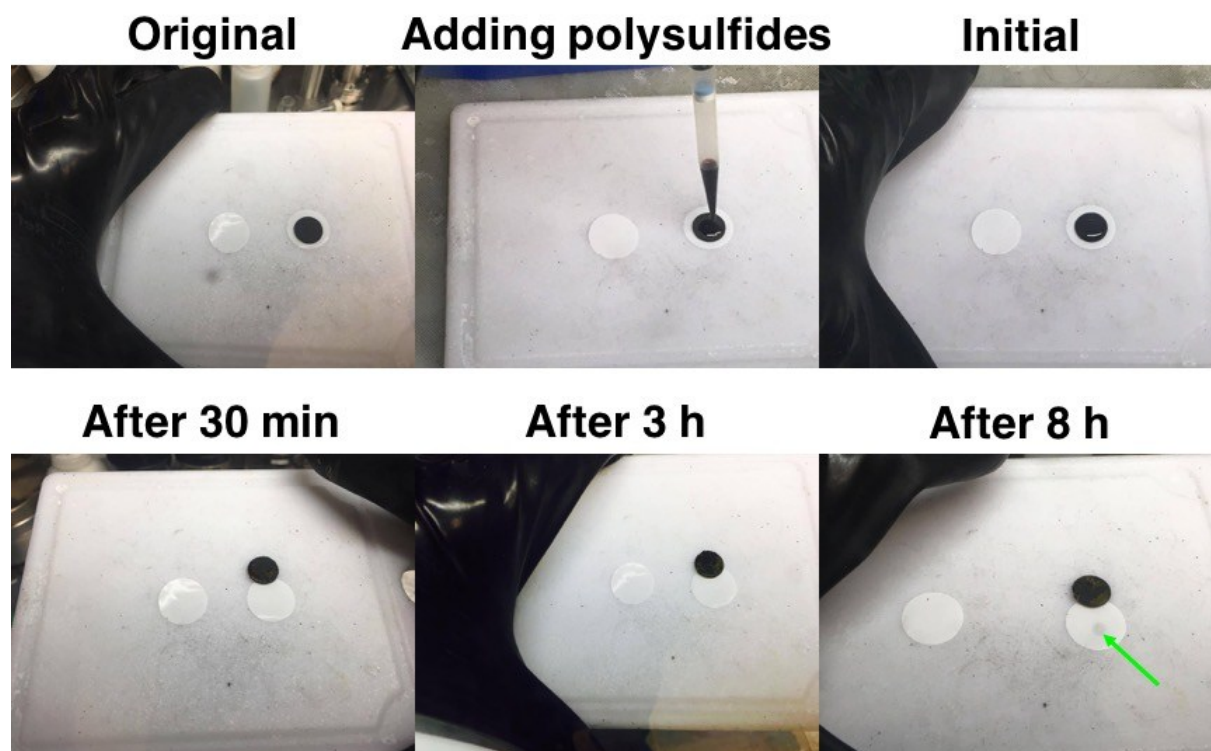


Fig. S14 Polysulfide-trapping capabilities of tandem cathodes during 8 h.

A pure carbon-based tandem electrode that contains no active material was prepared to examine the polysulfide-trapping capability of the electrode configuration (Fig. S14). To investigate the polysulfide-trapping capability, 250 μL of polysulfide, which is equal to 18.24 mg sulfur, was dropped onto the pure carbon tandem electrode. It is evident that the polysulfides were absorbed into the tandem electrode after 30 min; however, they still failed to penetrate through the electrode configuration to reach the polymeric separator even after 3 h. After 8 h, barely a minimum amount of polysulfides (green arrow) can escape from the electrode and reach the separator. This *ex-situ* polysulfide-trapping experiment indicates that the tandem cathode design effectively retains the polysulfides within the cathodes.

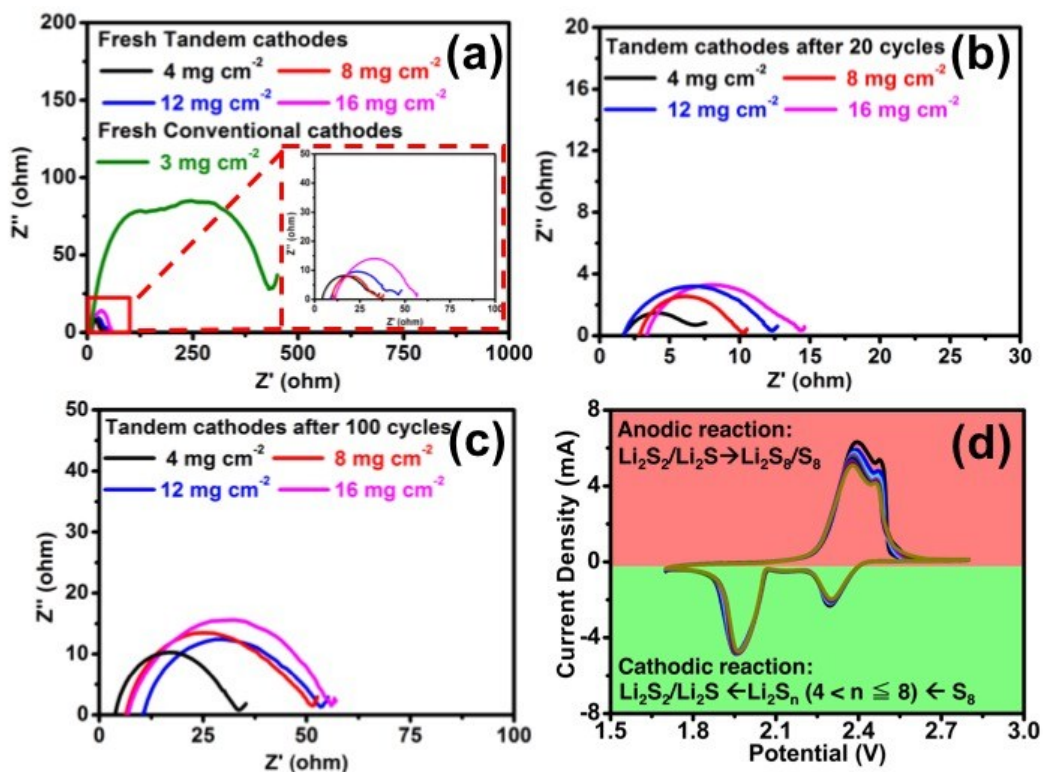


Fig. S15 EIS spectra of Li-S cells using the tandem cathodes with various sulfur loadings after different cycle numbers: (a) 0 cycle, the uncycled cells (the control cell included), (b) after 20 cycles, and (c) after 100 cycles. (d) The CV curves of Li-S cells using the tandem cathode with a sulfur loading of 4 mg cm⁻² in 10 cycles.

The EIS spectra of the uncycled Li-S cells employing the tandem cathodes with various sulfur loadings reveal that the cathode design effectively limits the build-up of resistance (Fig. S15a). The resistances of the cathodes slightly increase from 39 to 62 ohms. The modest increase could be attributed to the significant increase in sulfur loadings. The internal resistance diminished after 20 cycles (Fig. S15b). The results confirm that the rearranged active material occupied the optimized electrochemical spaces, in which the trapped active material was tightly entangled by the conductive carbon matrix and so had intimately contacted the electrolyte-channel network.^{S4,S5} After 100 cycles, the charge-resistance still remains at low values (< 70 ohms), indicating that the cathode architecture not only effectively retards the polysulfide migration but also reutilizes/reactivates the trapped

active material during cycling (Fig. S15c). The slight increase can be attributed to the formation of mossy Li and deactivated Li.

The tandem cathode with the sulfur loading of 4 mg cm^{-2} was used to demonstrate the redox reaction in the Li-S system (Fig. S15d). The overlapping CV curves suggest the excellent electrochemical reversibility. The exceptional performance may be attributed to the superior polysulfide retention and electrochemical reversibility of the tandem cathode.

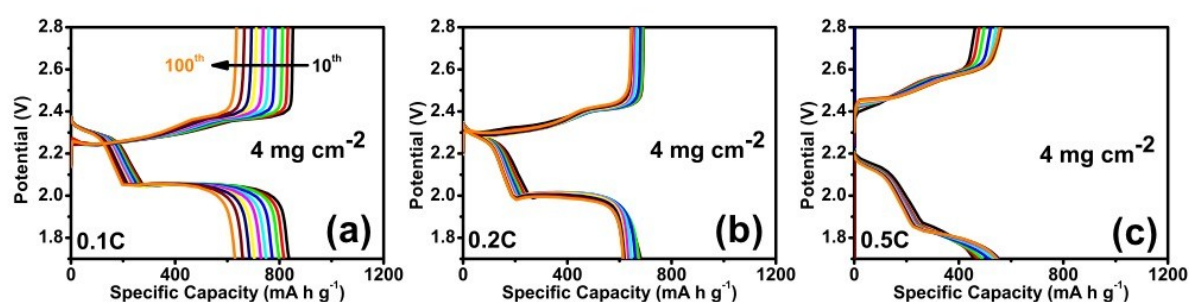


Fig. S16 Discharge/charge profiles of the Li-S cells employing the tandem cathodes with a sulfur loading of 4 mg cm^{-2} at various cycling rates: (a) 0.1C, (b) 0.2C, and (c) 0.5C rates.

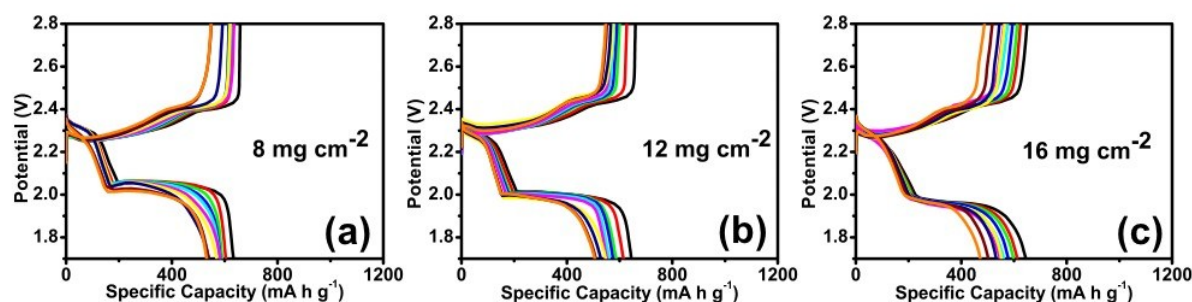


Fig. S17 Discharge/charge profiles of the Li-S cells employing the tandem cathodes with various sulfur loadings at 0.1C rate: (a) 8 mg cm^{-2} , (b) 12 mg cm^{-2} , and (c) 16 mg cm^{-2} .

The voltage profiles of the tandem cathodes with 4 mg cm^{-2} sulfur at various cycling rates and with 8, 12, and 16 mg cm^{-2} sulfur at 0.1C are, respectively, shown in Fig. S16 and Fig. S17. All profiles demonstrate the typical two-step redox reactions of sulfur. We also notice that at the faster cycling rate (*e.g.*, 0.5C rate), the discharge capacity gradually

increased to the peak capacity during the initial activation process, as shown in Fig. S16c and Fig. 6a. The activation process might result from that the sulfur cathodes with ultra-high loadings have insufficient time to trigger the redox reactions for all the embedded sulfur particles at the faster cycling rate, leading to the relatively low initial capacity.^{S6} In subsequent cycles, the unreacted sulfur clusters would be slowly activated so that the cell could reach the peak discharge capacity.

For the tandem cathodes with high sulfur loadings, the discharge/charge profiles at 0.1C rate show that even as the sulfur loadings significantly boost, the Li-S cells barely have a slight increase in polarization (Fig. S17). It is the special tandem cathode design that can reduce the built-up of resistance, which agrees with the EIS results. Moreover, the overlapping upper-discharge plateaus demonstrate the outstanding polysulfide-trapping capability and electrochemical stability. The long lower-discharge plateaus without dramatic shrinkages imply superior electrochemical accessibility and reversibility.^{S5}

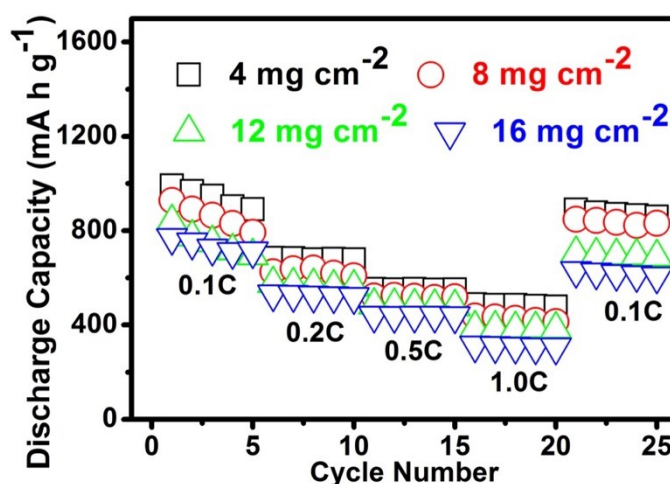


Fig. S18 Rate performance of the Li-S batteries employing the tandem cathodes with various sulfur loadings.

Fig. 18 shows the good rate performance of the Li-S cells employing tandem cathodes with different sulfur loadings of 4, 8, 12, and 16 mg cm⁻² from 0.1C to 1.0C rate, indicating the

superior reaction capability. As the cycling rates were changed back to 0.1C rate, the cells with sulfur loadings of 4, 8, 12, and 16 mg cm⁻² are still able to deliver high discharge capacities of, respectively, 900, 850 700, and 630 mA h g⁻¹.

S loading [mg cm ⁻²]	S content [%]	Initial areal capacity [mA h cm ⁻¹]	After cycling [mA h cm ⁻¹]	Capacity retention [%]	Flexibility	Ref.
18.1 ^{a)}	50 - 55	14.9 ^{b)}	12.1 ^{c)}	81	x	S7
11.4 ^{d)}	56	11.3	7.4	65	x	S8
4	60	4.0	2.5	63	v	This work
8	60	7.5	4.3	57	v	
12	60	10.1	6.1	60	v	
16	60	12.3	7.7	62	v	

Table S1 Comparison with the previous work.

a) polysulfides as the active material; b) 3rd cycle; c) 75th cycle; d) the active material was spread onto each layer

Table S2 Composition of each conducting layer and active-material layer.

	Materials ^{a)}	Mass ^{b)} [mg]	Mass ^{c)} [mg]
Conducting layer	CNF	63.5	177.2
	Sulfur	254.0	708.0
Active-material layer	SWCNT	10.0	27.8
	CNF	100.0	278.7

a) all materials were used as-received; b) regular size of 63.5 cm⁻²; c) large size of 177 cm⁻²

- S1 L. Li, Z. P. Wu, H. Sun, D. Chen, J. Gao, S. Suresh, P. Chow, C. V. Singh, N. Koratkar, *ACS Nano* **2015**, *9*, 11342.
- S2 R. Singhal, S.-H. Chung, A. Manthiram, V. Kalra, *J. Mater. Chem. A* 2015, **3**, 4530.
- S3 Z. Yuan, H.-J. Peng, J.-Q. Huang, X.-Y. Liu, D.-W. Wang, X.-B. Cheng, Q. Zhang, *Adv. Funct. Mater.* 2014, **24**, 6105.
- S4 C.-H. Chang, S.-H. Chung, A. Manthiram, *Small* 2016, **12**, 174.
- S5 S.-H. Chung, C.-H. Chang, A. Manthiram, *Small* 2016, **12**, 939.
- S6 S.-H. Chung, P. Han, A. Manthiram, *ACS Appl. Mater. Interfaces* 2016, **8**, 4709.
- S7 L. Qie, C. Zu, A. Manthiram, *Adv. Energy Mater.* 2016, **6**, 1502459.
- S8 L. Qie, A. Manthiram, *Adv. Mater.* 2015, **27**, 1694.